Desalination and Water Treatment
www.deswater.com
doi: 10.1080/19443994.2015.1060538

57 (2016) 13760–13769
June

Taylor & Francis
Taylor & Francis Group

Control of aluminium in treated water after defluoridation by electrocoagulation and modelling of adsorption isotherms

Richa Sinha, Sanjay Mathur*

Department of Civil Engineering, Malaviya National Institute of Technology, Jaipur 302017, India, Tel. +91 7877290494; email: richamnit10@gmail.com (R. Sinha), Tel. +91 9549654213; email: smathur.ce@mnit.ac.in (S. Mathur)

Received 3 February 2015; Accepted 4 June 2015

ABSTRACT

The removal of fluoride from drinking water by use of aluminium compounds is more prevalent than other defluoridation techniques due to the strong affinity between aluminium and fluoride. Electrocoagulation (EC) with aluminium electrodes is one such technique which is successfully used for defluoridation of water. But various monomeric and polymeric hydroxyl species of aluminium and fluoride complexes are formed in the process. In the recent past, the adverse effects of aluminium have been recognized. The present study was carried out to control aluminium content in water after defluoridation by EC process. In the present study, the aluminium content after EC was in the range of 6.2–48.5 mg/L, which was brought down to range 11.25–14.99 mg/L through optimized energy usage and further brought down to 0.030–0.149 mg/L with use of bentonite as coagulant.

Keywords: Defluoridation; Aluminium control; Coagulation; Optimization and adsorption isotherm

1. Introduction

Presence of fluorides in groundwater is a major problem in many parts of the world including India. Detrimental effects of fluorides depend upon the concentration and exposure [1]. Aluminium-based compounds have been used for defluoridation of water because of high affinity between aluminium and fluorine. Electrocoagulation (EC) with aluminium electrodes has been demonstrated as an efficient process for defluoridation [2–5]. This process involves applying electric current to sacrificial electrodes inside an electrolytic cell where the current generates a coagulating agent and gas bubbles [6]. The advantages of electrocoagulation include high particulate removal efficiency, compact treatment facility and possibility of complete automation [7].

Aluminium was earlier regarded as a relatively innocuous element, but in the recent past, researchers have found that its various bond forms with fluoride and other inorganic/organic ions are toxic in nature. Aluminium is a potential neurotoxic agent in human beings and researchers like Strunecka and Patocka [8] and Gauthier et al. [9] have elucidated synergistic effects of aluminium and fluorides and its role in Alzheimer's disease.

A little information is available in literature about the residual aluminium content after use of EC for defluoridation of water and its removal. The present study was carried out to control aluminium content in water after defluoridation by the EC process. It has been observed that the aluminium content in

*Corresponding author.

defluoridated water depends on the energy input. Thus, the task was to use minimum energy to bring down fluoride concentration below permissible limits of 1 mg/L (IS10500 regulations) [10]. The aluminium content in water was brought down appreciably with minimum energy input but it was still more than permissible levels of aluminium in drinking water (0.2 mg/L, IS10500 standards) [10]. In the next step, the efficiency of aluminium flocs removal was improved through coagulation with bentonite clay to bring down aluminium content. In the present study, the aluminium content after EC was in the range of 6.2–48.5 mg/L, which was brought down to range 11.25–14.99 mg/L through optimized energy usage and further brought down to 0.030–0.149 mg/L with use of bentonite.

2. Materials and method (fluoride removal)

A reactor of two-litre effective volume was used to conduct the batch experiments. Two aluminium electrodes with the purity of 98.99% and dimensions (84 mm width, 71 mm height and 2.5 mm thickness) were used. Electrodes were connected to a DC power supply (Testronix, 230 V DC) in monopolar configuration and a variable transformer was used to control the current intensity. Fluoride-containing samples were synthetically prepared in the laboratory by mixing NaF and NaCl (as supporting electrolyte) in tap water. The electrical conductivity of the prepared samples was measured and was set in the range 0.99–1.01 mS/cm. Initial pH of the solution was adjusted to 6 using HCl for all experiments. Magnetic stirrer was used to ensure complete mixing. All the experiments were accomplished at room temperature. Fluoride concentration was determined using ion selective electrode method [11] with a fluoride selective electrode (Thermo Scientific Orion 5-Star meter, 9609BNWP fluoride electrode). Conductivity and pH of the samples was measured using a calibrated conductivity meter (Lutron CD 4302) and pH meter (Haana HI-98128) respectively.

Table 1
Orthogonal array for L27 (3^3) Taguchi design

	Operating parameters			Responses	
S. no	Initial fluoride (F) (mg/l)	Applied current (*i*) (A)	Electrolysis time (*t*) (min)	Residual fluoride (mg/l)	Residual Al (mg/l)
1	2	0.31	10	1.12	9.4
2	2	0.31	30	0.31	19.48
3	2	0.31	50	0.23	28.12
4	2	0.53	10	0.71	10.6
5	2	0.53	30	0.36	26.12
6	2	0.53	50	0.09	47.04
7	2	0.75	10	0.61	14.9
8	2	0.75	30	0.18	33.48
9	2	0.75	50	0.01	48.5
10	5	0.31	10	1.56	6.2
11	5	0.31	30	0.71	12.1
12	5	0.31	50	0.29	18.05
13	5	0.53	10	1.42	7.81
14	5	0.53	30	0.25	17.5
15	5	0.53	50	0.19	27.6
16	5	0.75	10	1.27	9.25
17	5	0.75	30	0.14	25.8
18	5	0.75	50	0.11	39.45
19	8	0.31	10	3.40	6.07
20	8	0.31	30	1.35	10.53
21	8	0.31	50	0.60	17.5
22	8	0.53	10	2.30	6.53
23	8	0.53	30	0.56	15.79
24	8	0.53	50	0.30	25.75
25	8	0.75	10	1.37	10
26	8	0.75	30	0.38	23.68
27	8	0.75	50	0.23	40.42

The study for fluoride removal was conducted using Taguchi method of design of experiments (MINITAB 14). The operating parameters studied were initial fluoride concentration (2, 5 and 8 mg/L), applied current (0.31, 0.53 and 0.75 A) and electrolysis time (10, 30 and 50 min) for two responses: residual fluoride and residual aluminium. The data has been summarized in Table 1. The residual aluminium presented in Table 1 includes both dissolved and bind forms of aluminium.

The relationship between residual fluoride and residual aluminium with combination of control factors is obtained using non-linear regression analysis with the help of SYSTAT 7.0 software as shown below in Eqs. (1) and (2). The data in Table 1 is normalized and used for developing the equations. The data is normalized by dividing each value with the maximum existing value in the column. The correctness of the calculated constants (in equations given below) is confirmed by high correlation coefficients (R^2) in the tune of 0.95 and above. Thus the presented model is considered suitable to be used for further analysis.

$$\begin{aligned}\text{Residual fluoride} = {} & 0.608 + (0.741 \times \mathrm{F}) - (0.557 \times i) \\ & - (1.3 \times t) - (0.559 \times \mathrm{F} \times i) \\ & + (0.424 \times i \times t) - (0.622 \times \mathrm{F} \times t) \\ & + \left(0.261 \times \mathrm{F}^2\right) + \left(0.251 \times i^2\right) \\ & + \left(0.760 \times t^2\right)\end{aligned} \tag{1}$$

$$\begin{aligned}\text{Residual aluminium} = {} & 0.291 - (0.734 \times \mathrm{F}) - (0.09 \times i) \\ & + (0.242 \times t) - (0.01 \times \mathrm{F} \times i) \\ & + (0.757 \times i \times t) \\ & - (0.322 \times \mathrm{F} \times t) + \left(0.549 \times \mathrm{F}^2\right) \\ & + \left(0.071 \times i^2\right) + \left(0.024 \times t^2\right)\end{aligned} \tag{2}$$

It is evident from Table 1, that the residual aluminium in defluoridated water varies from 9.2 to 48.2 mg/L, which is much higher than permissible standards of aluminium in drinking water, and hence requires further treatment.

3. Aluminium control

3.1 Control of aluminium by optimization of energy input

As first step, to control aluminium after EC process, the energy input has been minimized to bring residual fluoride in water below 1 mg/L. In the present work, the target value of fluoride in treated water was kept as 0.7 mg/L. The energy input depends on applied current (i) and electrolysis time (t). The optimum values of "i" and "t" for target value of fluoride as 0.7 mg/L were determined for each initial fluoride concentration using grid search method, programmed in FORTRAN. The grid search method calculates the minimum point of a multi-variable function using the grid search. The multidimensional grid has a centroid which locates the optimum point. The search involves multiple passes. In each pass, the method locates a node (point of intersection) with the least function value. This node becomes the new centroid and builds a smaller grid around it. Successive passes end up shrinking the multidimensional grid around the optimum [12]. The value of minimum applied current and electrolysis time for each initial fluoride concentration was calculated by the program and has been presented in Table 2 (columns 2 and 3). The respective values for residual aluminium were calculated by Eq. (2) and have been presented in Table 2 (column 4).

It is apparent from Table 2 that the residual aluminium in water after energy optimization for EC is still higher than permissible limit (0.2 mg/L) and needs further removal.

3.2. Aluminium control by plain flocculation, settling and filtration

To control the aluminium content in treated water flocculation, settling and filtration was attempted for all the optimized sets. After the EC process is completed, the sample was stirred for 20 min at 10 rpm and settled for 30 min. The supernatant was further filtered by 2.2 μm filter (Whatman Grade 42) and the residual aluminium concentration was measured. The results are shown in Table 3. The pH measured after filtration is in the range of 6.52–7.13; at this pH range, the aluminium has minimum solubility, [13] which indicates that majority of aluminium present in water is contributed by aluminium hydroxide flocs formed during electrolysis. The turbidity of the samples was in the range of 4.8–6.9 NTU, which also confirms the hypothesis pertaining to presence of aluminium in bind forms. Therefore, it was necessary to remove these flocs efficiently to reduce the aluminium concentration in water.

It is apparent from Table 3 that aluminium content in water after flocculation, settling and filtration (without coagulant aid) is still more than the permissible limits. Thus, to improve settling efficiency, bentonite clay was used as coagulant aid followed by flocculation, settling and filtration.

Table 2
Details of optimized sets (minimum value of applied current and time for target value of residual fluoride as 0.7 mg/L)

	Operating parameters			Aluminium after EC (mg/L)	
Set no.	Initial fluoride (mg/L)	Applied current (A)	Electrolysis time (min)	Predicted	Experimental
1	2	0.33	17.05	13.659	14.018
2	3	0.32	20.93	12.097	12.723
3	4	0.39	22.41	11.596	11.926
4	5	0.36	27.85	11.304	11.732
5	6	0.32	34.90	11.249	11.586
6	7	0.31	41.08	12.204	12.504
7	8	0.37	43.84	14.990	I5.320

Table 3
Residual aluminium concentration after settling, flocculation and filtration (without coagulant aid)

Set no.	Initial fluoride concentration (mg/L)	Aluminium after EC (mg/L)	Aluminium after plain settling, flocculation and filtration (mg/L)
1	2	14.018	0.384
2	3	12.723	0.357
3	4	11.926	0.295
4	5	11.732	0.276
5	6	11.586	0.252
6	7	12.504	0.384
7	8	15.320	0.403

3.3. Control of aluminium by use of bentonite clay

Bentonite, which is predominantly montmorillonite clay, is characterized by one aluminium octahedral sheet placed between two Si tetrahedral sheets. Bentonite is negatively charged, all the positively charged aluminium species are adsorbed by bentonite. The layered structure of the clay expands after wetting. Na^+ and Ca^{2+} are strongly hydrated in the presence of water, resulting in a hydrophilic environment at the bentonite surface [14]. Bentonite disperses into colloidal particles and provides large surface area per unit weight of clay [15]. When bentonite disaggregates in water, swelling takes place and hence the available surface area increases [15]. This large surface area provides greater contact opportunity and leads to destabilization by charge neutralization. The second advantage of using bentonite is improvement of floc properties. It adds weight to the flocs and causes them to settle more rapidly than flocs containing mostly Al $(OH)_3$. Bentonite is cheaper than chemicals and it fulfils the economic benefits of the operators as well as environmental concerns [16]. Moreover, commercially available chemical coagulants may create adverse impacts on the treated water quality, which gives an edge to bentonite clay over other coagulants [17].

The experimental investigations were carried out to determine appropriate flocculation time. These investigations were performed for set nos. 1, 4 and 7 (Table 2). The dose of bentonite (1 g/L) and settling time (30 min) was kept constant, while the flocculation time was varied from 10–30 min. It is evident from Fig. 1 that 20 min flocculation time gave better removal efficiency. Therefore, it was kept constant for all experiments.

Bentonite clay was added after EC process, and mixed thoroughly for 1 min at 40 rpm. This was followed by flocculation (20 min) and settling (30 min). The supernatant was filtered (2.2 μm filter) and analysed for remaining aluminium. The experimental study was designed using 4-level Taguchi design method. The operating parameters were aluminium after EC (11.586, 12.723, 14.018 and 15.320 mg/L) and bentonite dose (1, 2, 3 and 4 g/L) for estimation of response (aluminium after bentonite dosing). MINITAB 14 software was used for analysis of results. A total set of 16 experiments were performed. The experiments were performed in duplicate sets and the average results have been reported in the Table 4. It can be observed that aluminium concentration was within permissible limit for all the applied doses of

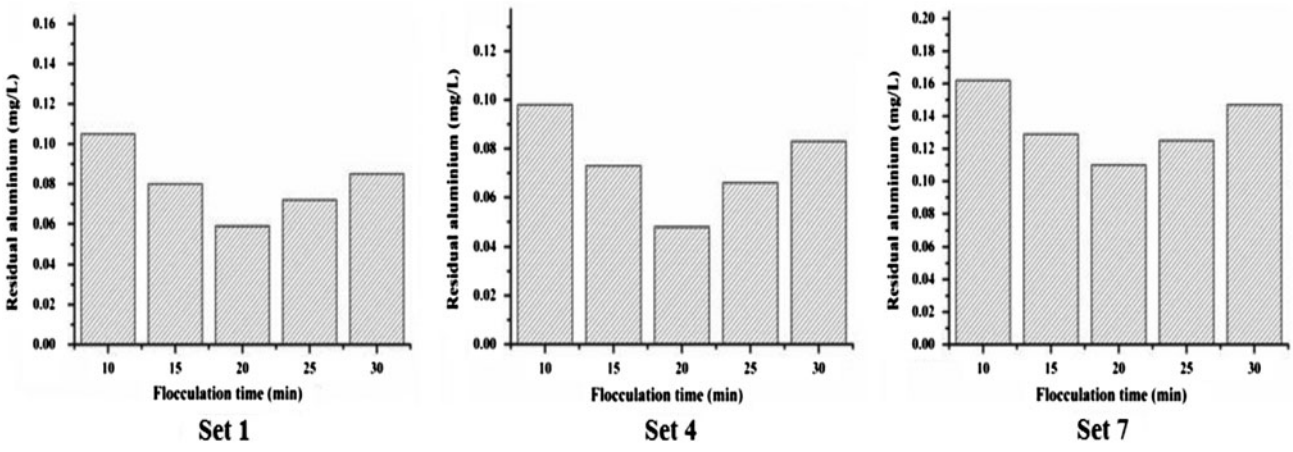

Fig. 1. Effect of flocculation time on residual aluminium after bentonite dosing (set 1, 4, 7).

Table 4
Orthogonal array for L16 (2^4) Taguchi design

S. no.	Operating parameters		Response
	Aluminium after EC Al_{EC} (mg/L)	Bentonite dose D_b (g/L)	Aluminium after bentonite dosing Al_{bd} (mg/L)
1	11.586	1	0.048
2	11.586	2	0.030
3	11.586	3	0.037
4	11.586	4	0.053
5	12.723	1	0.054
6	12.723	2	0.044
7	12.723	3	0.050
8	12.723	4	0.060
9	14.018	1	0.059
10	14.018	2	0.072
11	14.018	3	0.087
12	14.018	4	0.101
13	15.320	1	0.110
14	15.320	2	0.080
15	15.320	3	0.130
16	15.320	4	0.149

bentonite. Maximum removal was observed at the dose of 2 g/L. The pH after EC was in range of 6.32–6.90. After addition of bentonite, flocculation, settling and filtration; pH was in range of 7.13–7.24. The turbidity of the samples after filtration was in the range of 1.3–2.6 NTU, which suggests that the flocs have been efficiently settled.

The adequacy of the model was assessed through ANOVA. High R^2 value of 93.55% indicates the validity of the model (Table 5).

The expression to calculate residual aluminium after bentonite dosing was developed by using normalized values of data in Table 4. Normalization was done by dividing each value in the column by maximum value of the column. SYSTAT 7.0 was used for this purpose and the expression is presented in Eq. (3).

$$\begin{aligned} Al_{bd} = {} & 4.435 - (9.893 \times Al_{EC}) - (2.235 \times D_b) \\ & + (1.828 \times Al_{EC} \times D_b) + \left(6.174 \times Al_{EC}^2\right) \\ & + (0.698 \times D_b^2) \end{aligned} \quad (3)$$

To verify the correctness of the equations obtained, actual vs. predicted response graphs were plotted. Fourteen sets of experiments as mentioned in Table 6 were performed to verify the equations. The graphs and their respective R^2 value are displayed in the Fig. 2.

Table 5
ANOVA table for residual aluminium after bentonite dosing

Source	DF	Seq. SS	Adj. SS	Adj. MS	F	P
Aluminium after plain settling	3	186.067	186.067	62.022	37.06	0.000
Bentonite dose	3	32.369	32.369	10.790	6.45	0.013
Error	9	15.064	15.064	1.674		
Total	15	233.500				

S = 1.29373 R-Sq. = 93.55%

Table 6
Operational parameter settings and their respective experimental and predicted responses

	Operational parameters		Aluminium after bentonite dosing (mg/L)	
S. no.	Aluminium after EC (mg/L)	Bentonite dose (g/L)	Predicted	Experimental
1	11.586	2	0.035	0.030
2	11.732	2	0.035	0.032
3	11.926	2	0.036	0.036
4	12.504	2	0.041	0.040
5	12.723	2	0.044	0.044
6	14.018	2	0.066	0.072
7	15.320	2	0.102	0.080
8	15.320	4	0.150	0.150
9	14.018	4	0.102	0.102
10	14.018	3	0.077	0.078
11	11.586	3	0.035	0.036
12	12.504	1	0.049	0.053
13	11.926	1	0.047	0.050
14	12.504	1	0.049	0.053

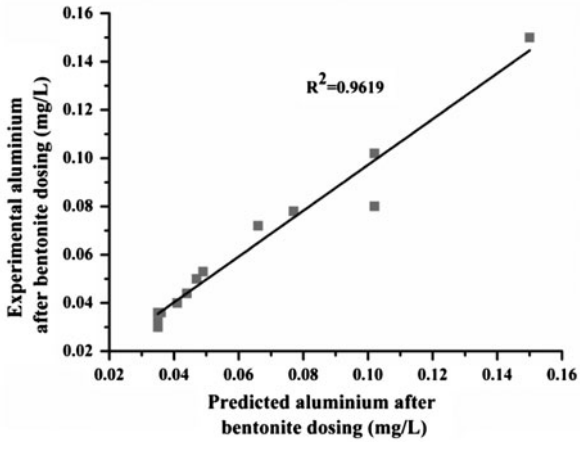

Fig. 2. Experimental vs. predicted values for aluminium after bentonite dosing.

4. Adsorption isotherms

The experimental data were fitted with Langmuir, Freundlich and Redlich–Peterson isotherms. Isotherms were calculated using optimized set of results. Set of seven varying initial fluoride concentrations and their respective aluminium concentration after EC (C_0) were used for calculations. The amount of aluminium adsorbed by bentonite was determined using a mass balance equation expressed in Eq. (4) [18].

$$q_e = V\frac{(C_0 - C_e)}{W} \tag{4}$$

where q_e is aluminium concentration adsorbed on the bentonite (mg/g), C_e is aluminium concentration in solution (mg/L), C_0 is aluminium concentration in

Table 7
Data used to determine the highest fitted isotherm

Aluminium after EC (mg/L) (C_0)	Aluminium after bentonite (mg/L) (C_e)	Aluminium adsorbed on bentonite (mg/g) (q_e)	$q_{pred.}$		
			Langmuir $q_e = \frac{q_{max} K_L C_e}{1+K_L C_e}$	Freundlich $q_e = K_F C_e^{1/n}$	Redlich–Peterson $q_e = \frac{AC_e}{1+BC_e^g}$
11.586	0.030	11.556	11.334	11.472	11.470
11.732	0.032	11.700	11.601	11.667	11.667
11.926	0.036	11.890	12.074	12.032	12.034
12.504	0.040	12.464	12.481	12.369	12.372
12.723	0.044	12.679	12.835	12.681	12.685
14.018	0.072	13.946	14.428	14.424	14.423
15.320	0.080	15.240	14.715	14.827	14.823

solution after EC (mg/L), V is volume of solution used (L) and m is mass of bentonite used (g). The dose of 2 g/L was the optimized dose of bentonite, and used for calculation of presented isotherms. The experimental q_e was calculated by Eq. (4) and the predicted q_e is obtained from the non-linear expressions of Langmuir [19] Freundlich [20] and Redlich–Peterson [21] isotherms as shown in Table 7. In the case of the non-linear method, a trial-and-error procedure was developed to determine the isotherm parameters using an optimization routine to maximize the coefficient of determination between the experimental data and isotherms [22]. This was performed in the solver add-in with Microsoft's spreadsheet, Microsoft Excel. The protocol which has been used is, experimental data was manually entered in MS-Excel, the formulated algorithm was carried out and the predicted curve was overlaid on the experimental data points, and goodness of fit was observed [23].

Goodness of fit is an essentially important parameter that estimates how well the curve (i.e. the prediction) pronounces the experimental data. The following parameters are measured and judged for the goodness of fit:

Coefficient of determination (R^2): the coefficient of determination is such that $0 < R^2 < 1$, and denotes the strength of the linear association between experimental data, $q_{e.exp.}$, and prediction data, $q_{e.pred}$. The coefficient of determination represents the percent of the experimental data that is the closest to the line of best fit. R^2 is described by the expression in Eq. (5) [24]:

$$R^2 = 1 - \frac{\sum_{n=1}^{n}(q_{e.exp.n} - q_{e.pred.n})\text{^}2}{\sum_{n=1}^{n}(q_{e.exp.n} - \overline{q_{e.exp.n}})\text{^}2} \quad (5)$$

where $q_{e.exp}$ is the equilibrium sorption capacity found from the batch experiment, $q_{e.pred.}$ is the prediction from the isotherm model for corresponding to C_e and n is the number of observations.

Residual root mean square error (RMSE) and the chi-square test (χ^2): The small values of RMSE and χ^2 indicate the better model fitting and the similarity of model with the experimental data, respectively [25]. The standard equations are as follows [24]:

$$\text{RMSE} = \sqrt{\frac{1}{n-1}\sum_{n=1}^{n}(q_{e.exp.n} - q_{e.pred.n})\text{^}2} \quad (6)$$

$$\chi^2 = \sum_{n=1}^{n}\frac{(q_{e.exp.n} - q_{e.pred.n})\text{^}2}{q_{e.exp.n}} \quad (7)$$

The results for goodness of fit for the three isotherms have been presented in Table 8.

The R^2 values of Redlich–Peterson and Freundlich isotherms are almost similar. Redlich–Peterson isotherm has features of both Langmuir and Freundlich

Table 8
Isotherm parameters

Isotherm	Parameter	Values
Langmuir	q_{max} (mg/g)	17.923
	K_L (L/mg)	57.336
	RMSE	0.323
	χ^2	0.007
	R^2	0.9430
Freundlich	K_F (L/g)	28.707
	n	3.823
	RMSE	0.270
	χ^2	0.005
	R^2	0.9602
Redlich–Peterson	A (L/g)	39,677.65
	B (L/mg)	1,394.967
	g	0.744
	RMSE	0.270
	χ^2	0.005
	R^2	0.9600

[21]. The model has a linear dependence on concentration in the numerator and an exponential function in the denominator [26] to represent adsorption equilibria over a wide concentration range, which can be applied either in homogeneous or heterogeneous systems due to its versatility [27]. It approaches Freundlich isotherm model at high concentration (as the exponent g tends to zero) and is in accordance with the low concentration limit of the ideal Langmuir condition (as the g values are all close to one) [28].

In the present case, coefficient "g" = 0.744, which indicates that it is approaching Freundlich isotherm. Also, the Freundlich isotherm has the best fit if compared with Langmuir. This suggests that features of Freundlich isotherm are applicable to the present adsorption and its plot is shown in Fig. 3. So it can be concluded that it is non-ideal and reversible adsorption, not restricted to the formation of monolayer. This model can be applied to multilayer adsorption, with non-uniform distribution of adsorption heat and affinities over the heterogeneous surface [20]. The amount adsorbed is the summation of adsorption on all sites (each having bond energy), with the stronger binding sites occupied first, until adsorption energy is exponentially decreased upon the completion of adsorption process [29]. The slope ranges of Freundlich isotherm, between 0 and 1, is a measure of adsorption intensity or surface heterogeneity, becoming more heterogeneous as its value gets closer to zero. Whereas, a value below unity implies chemisorptions process, where $1/n$ above one is an indicative of cooperative adsorption [30]. The slope in the present study is 0.26, which is indicative of chemisorptions taking place.

5. Sludge analysis

XRD was performed for raw bentonite (Fig. 4) and on the sludge obtained in the process after using bentonite clay for aluminium control (Fig. 5). XRD patterns of raw bentonite indicate that it is mostly made up of montmorillonite, quartz and kaolinite. Chemically, montmorillonite is described as a hydrous aluminium silicate containing small amounts of alkali and alkaline-earth metals. XRD confirms that the metal present in bentonite used for this study is sodium and magnesium. Sodium bentonite swells or expands to a greater degree than its calcium equivalent and hence develops larger surface area [15].

The strongest peaks identified for sludge were of aluminium fluoride silicate, sodium aluminium fluoride. Other small peaks of sodium magnesium

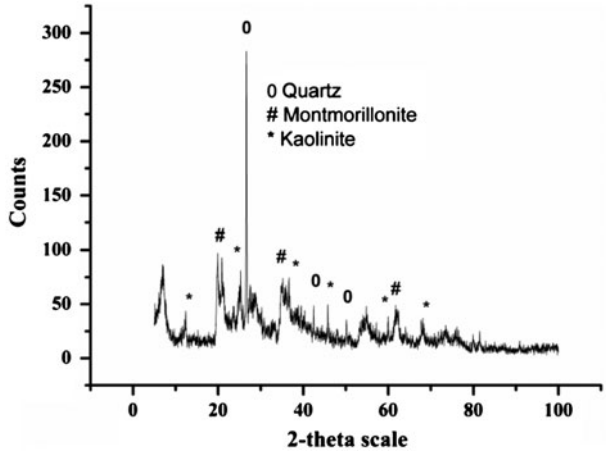

Fig. 4. XRD analysis of raw bentonite.

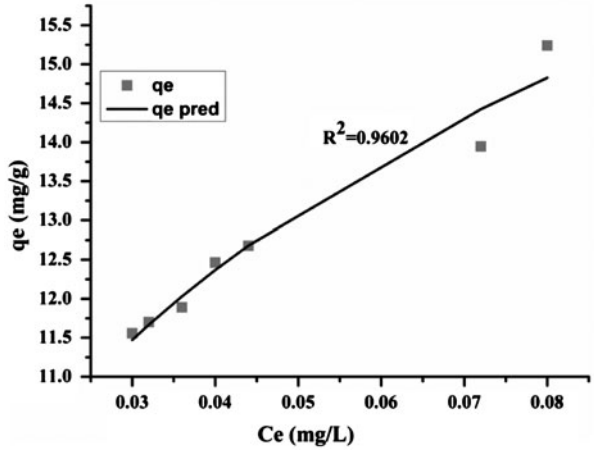

Fig. 3. Freundlich isotherm applied for aluminium remaining after benonite dosing.

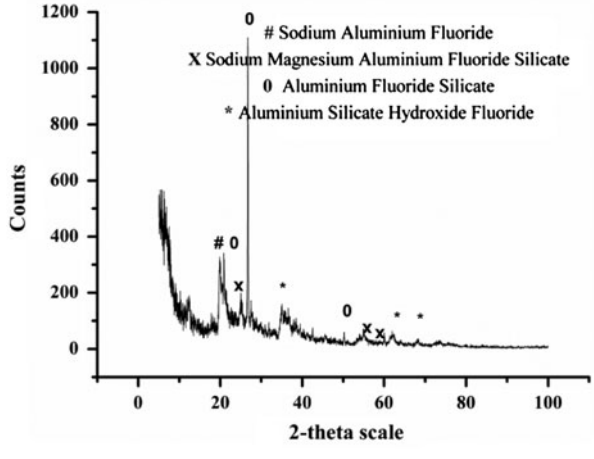

Fig. 5. XRD analysis of sludge produced in the EC process using Strategy C (F = 8 mg/l; i = 0.37 A; t = 43.84 min).

aluminium fluoride silicate and aluminium silicate hydroxide fluoride were also present. The formation of silicate compounds in sludge indicates the presence of bentonite clay particles. The presence of these compounds indicates the adsorption of alumino complexes in the form of flocs on to the bentonite clay particles, and hence verifies the role of bentonite clay in better settling of flocs formed in the EC process.

6. Conclusions

Successful defluoridation was achieved by EC method, but residual aluminium remaining in the treated was higher than permissible levels. The input parameter of EC process: applied current and electrolysis time, were minimized to control aluminium in the treated water. It was done using grid search program. Further, it was observed that appreciable reduction was achieved by flocculation, settling and filtration without using coagulant aid. However, to bring down the aluminium concentrations within permissible limit, bentonite clay was used. Use of bentonite was found effective in keeping aluminium concentration within permissible limits. The adsorption isotherm study reveals that the removal of aluminium by use of bentonite particles is chemisorption process. The aluminosilico-fluoro compound present in the sludge indicates towards the same.

References

[1] S. Vasudevan, B.S. Kannan, J. Lakshmi, S. Mohanraj, G. Sozhan, Effects of alternating and direct current in electrocoagulation process on the removal of fluoride from water, J. Chem. Technol. Biotechnol. 86 (2013) 428–436.
[2] N. Mameri, H. Lounici, D. Belhocine, H. Grib, D.L. Piron, Y. Yahiat, Defluoridation of Sahara water by small plant electrocoagulation using bipolar aluminium electrodes, Sep. Purif. Technol. 24 (2001) 113–119.
[3] M.M. Emamjomeh, M. Sivakumar, Fluoride removal by a continuous flow electrocoagulation reactor, J. Environ. Manage. 90 (2009) 1204–1212.
[4] N. Drouiche, S. Aoudj, H. Lounici, M. Drouiche, T. Ouslimane, N. Ghaffour, Fluoride removal from pretreated photovoltaic wastewater by electrocoagulation: An investigation of the effect of operational parameters, Proc. Eng. 33 (2012) 385–391.
[5] R. Sinha, A. Singh, S. Mathur, Multiobjective optimization for minimum residual fluoride and specific energy in electrocoagulation process, Desalin. Water Treat. (2014) 1–11, doi: 10.1080/19443994.2014.990929.
[6] S. Vasudevan, M.A. Oturan, Electrochemistry: As cause and cure in water pollution—An overview, Environ. Chem. Lett. 12 (2014) 97–108.
[7] S. Vasudevan, J. Lakshmi, G. Sozhan, Studies on a Mg–Al–Zn alloy as an anode for the removal of fluoride from drinking water in an electrocoagulation process, Clean—Soil, Air, Water 37 (2009) 372–378.
[8] A. Strunecka, J. Patocka, Pharmacological and toxicological effects of aluminofluoride complexes, Fluoride 32 (1999) 2–242.
[9] E. Gauthier, E. Fortier, F. Courchesne, P. Pepin, J. Mortimer, D. Gauvreau, Aluminum forms in drinking water and risk of Alzheimer's disease, Environ. Res. 84 (2000) 234–246.
[10] Indian Standard Drinking Water Specification IS10500, Bureau of Indian standards, New Delhi, 2012.
[11] L.S. Clesceri, A.E. Greenberg, A.D. Eaton (Eds.), Standard Methods for the Examination of Water and Wastewater, twentieth ed., APHA-AWWA-WEF, Washington, DC, 1998.
[12] Radha, M. Kumar, Location aware recommendation system, Int. J. Manage. Inf. Technol. Eng. 2 (2014) 43–52.
[13] P.T. Srinivasan, T. Viraraghavan, K.S. Subramanian, Aluminium in drinking water: An overview, Water Sa. 25 (1999) 47–55.
[14] Y.-H. Shen, Preparations of organobentonite using nonionic surfactants, Chemosphere 44 (2001) 989–995.
[15] A.G. Klem, R.W. Doehler, Industrial applications of bentonite, in: Symposium on Industrial Applications (Proceedings of the Tenth National Conference), October 16–18, 1961, Austin, Texas, pp. 272–283.
[16] M.H. Al-Qunaibit, W.K. Mekhemer, A.A. Zaghloul, The adsorption of Cu(II) ions on bentonite—A kinetic study, J. Colloid Interface Sci. 283 (2005) 316–321.
[17] A. Özcan, Ç. Ömeroğlu, Y. Erdoğan, A.S. Özcan, Modification of bentonite with a cationic surfactant: An adsorption study of textile dye Reactive Blue 19, J. Hazard. Mater. 140 (2007) 173–179.
[18] B.M. Vanderborght, R.E. Van Grieken, Enrichment of trace metals in water by adsorption on activated carbon, Anal. Chem. 49 (1977) 311–316.
[19] I. Langmuir, The constitution and fundamental properties of solids and liquids. Part I. Solids, J. Am. Chem. Soc. 38 (1916) 2221.
[20] H.M.F. Freundlich, Über die adsorption in lösungen (About the adsorption in solutions), Z. Phys. Chem.-Frankfurt 57A (1906) 385–470.
[21] O. Redlich, D.L. Peterson, A useful adsorption isotherm, J. Phys. Chem. 63 (1959) 1024.
[22] K.V. Kumar, Optimum sorption isotherm by linear and non-linear methods for malachite green onto lemon peel, Dyes Pigm. 74 (2007) 595–597.
[23] M.A. Hossain, H.H. Ngo, W. Guo, Introductory of Microsoft Excel solver function—Spreadsheet method for isotherm and kinetics modelling of metals biosorption in water and wastewater, J. Water. Sustainability 3 (2013) 223–237.
[24] M.A. Hossain, H.H. Ngo, W.S. Guo, T. Setiadi, Adsorption and desorption of copper(II) ions onto garden grass, Bioresour. Technol. 121 (2012) 386–395.
[25] Y.S. Ho, J.F. Porter, G. McKay, Equilibrium isotherm studies for the sorption of divalent metal ions onto peat: Copper, nickel and lead single component systems, Water, Air, Soil Pollut. 141 (2002) 1–33.
[26] J.C.Y. Ng, W.H. Cheung, G. McKay, Equilibrium studies of the sorption of Cu(II) ions onto chitosan, J. Colloid Interface Sci. 255 (2002) 64–74.

[27] F. Gimbert, N. Morin-Crini, F. Renault, P.M. Badot, G. Crini, Adsorption isotherm models for dye removal by cationized starch-based material in a single component system: Error analysis, J. Hazard. Mater. 157 (2008) 34–46.
[28] L. Jossens, J.M. Prausnitz, W. Fritz, E.U. Schlünder, A.L. Myers, Thermodynamics of multi-solute adsorption from dilute aqueous solutions, Chem. Eng. Sci. 33 (1978) 1097–1106.
[29] A.W. Adamson, A.P. Gast, Physical Chemistry of Surfaces, sixth ed., Wiley-Interscience, New York, NY, 1997.
[30] F. Haghseresht, G. Lu, Adsorption characteristics of phenolic compounds onto coal-reject-derived adsorbents, Energy Fuels 12 (1998) 1100–1107.